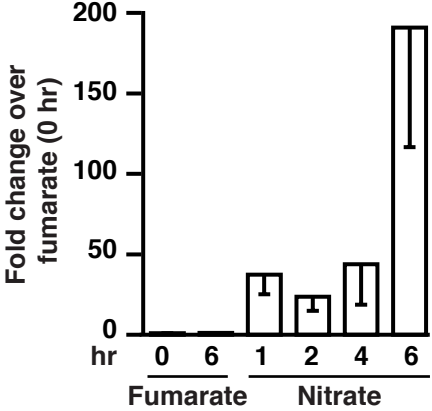


Figure S1

Seth *et al.*

A



B

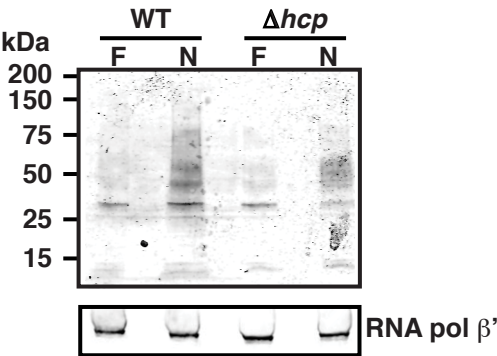
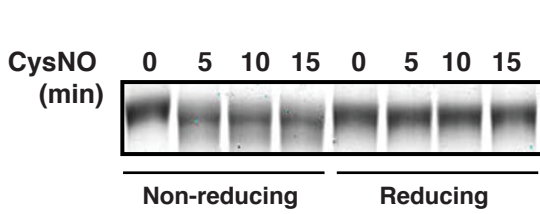


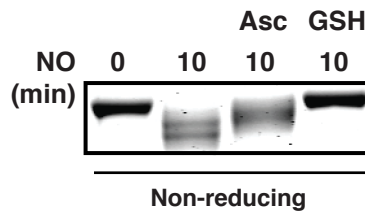
Figure S2

Seth *et al.*

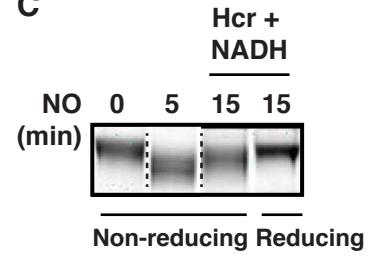
A



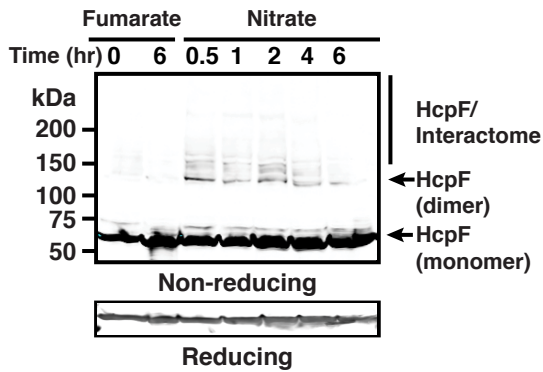
B



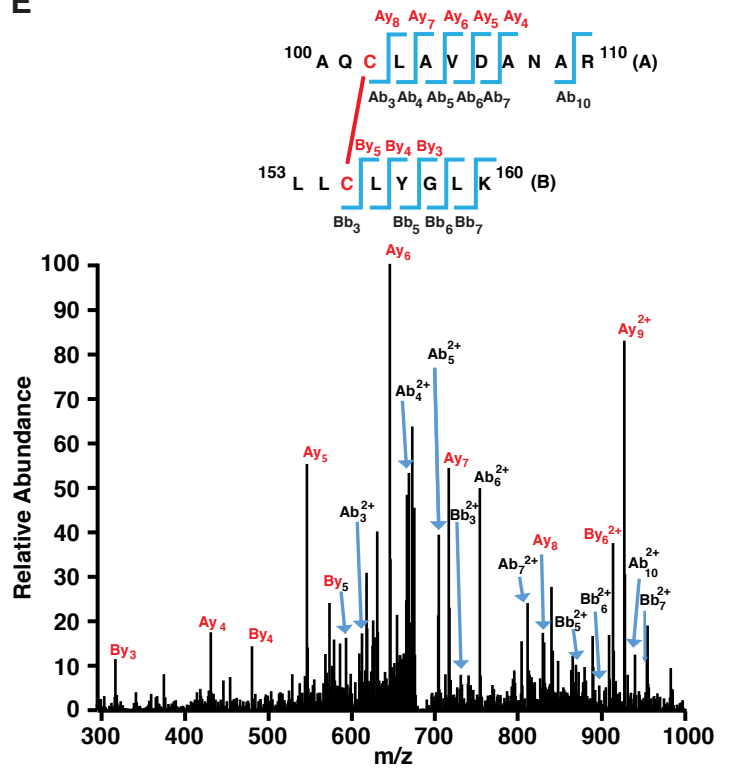
C



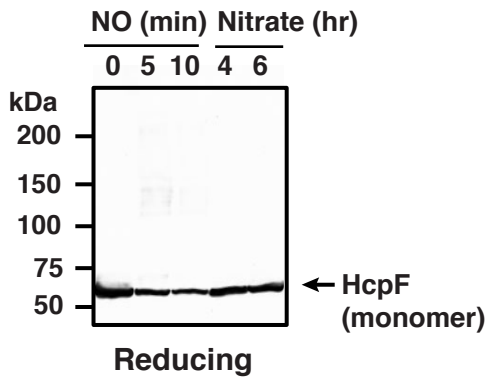
D



E



F



G

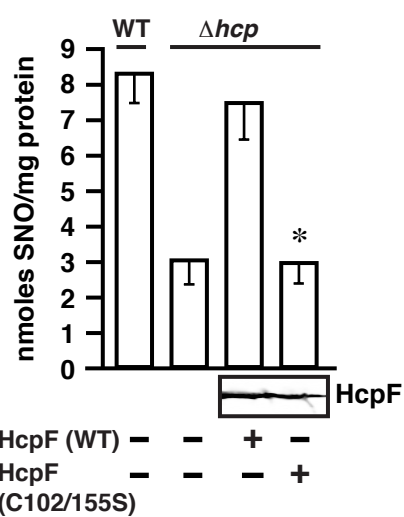
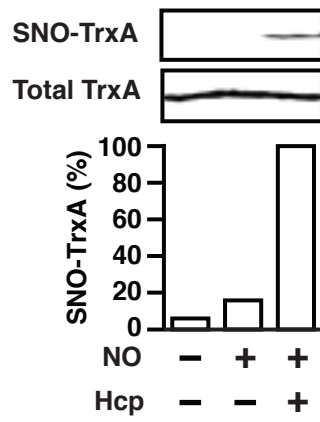


Figure S3
Seth *et al.*

A



B

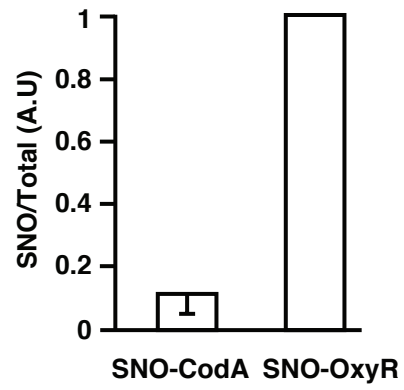
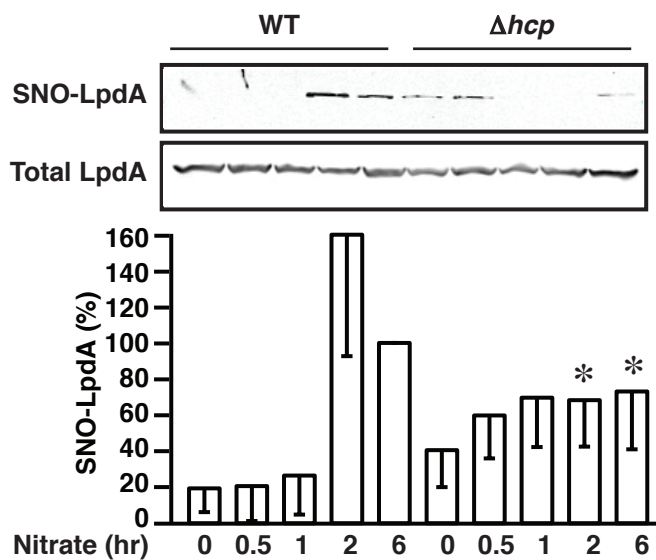


Figure S4

Seth *et al.*

A



B

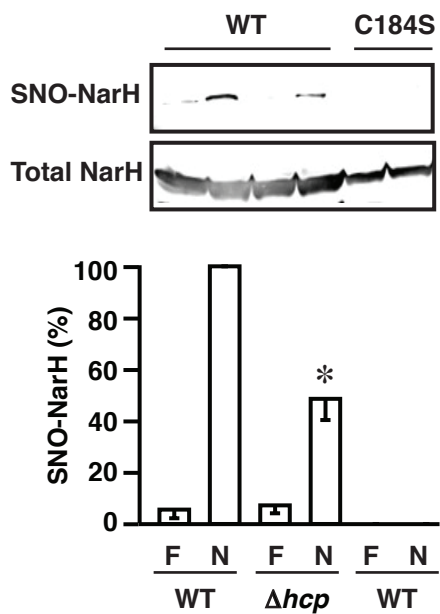
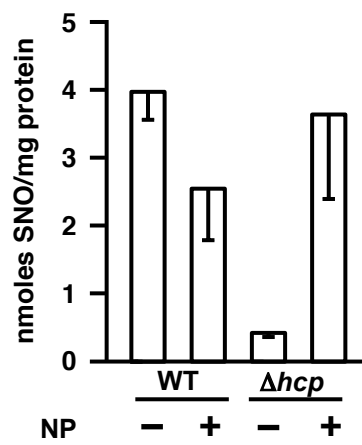


Figure S5
Seth *et al.*

A



B

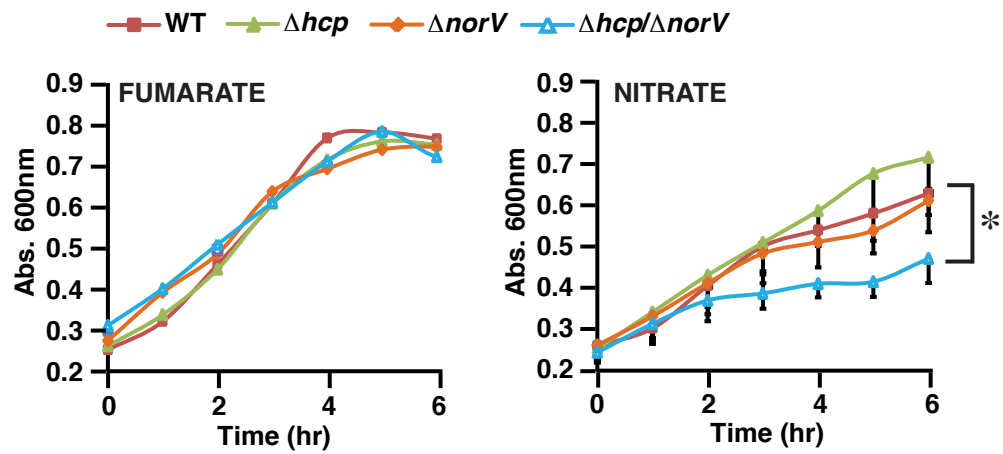


Table S1. Nitrosylation, Growth and Nitrite Measurements in *E. coli* Strains Mutant for OxyR-dependent, Nitrate-induced Genes During ARN, Related to Figure 1

Strain	Nitrosylation (nmoles/mg protein)	A600	Nitrite (mM)	Strain	Nitrosylation (nmoles/mg protein)	A600	Nitrite (mM)
<i>hcp</i>	0.58	0.98	6.10	<i>kgtP</i>	4.26	0.82	6.08
<i>ymgA</i>	1.63	1.23	6.37	<i>gst</i>	4.31	0.95	4.99
<i>ymgC</i>	2.11	1.15	6.38	<i>gcvP</i>	4.35	0.98	6.49
<i>ybaY</i>	2.20	1.09	6.75	<i>ynhG</i>	4.39	1.13	5.05
<i>yeaC</i>	2.26	1.08	6.94	<i>acnB</i>	4.43	0.79	4.23
<i>lpd</i>	2.53	0.83	7.59	<i>fdnH</i>	4.52	1.07	5.43
<i>yjcB</i>	2.56	0.99	6.30	<i>yobA</i>	4.54	0.96	6.00
<i>speD</i>	2.59	0.74	3.76	<i>fdoG</i>	4.58	1.12	6.50
<i>hslV</i>	2.69	0.95	5.40	<i>nuoI</i>	4.71	0.94	5.15
<i>tpx</i>	3.03	1.29	6.54	<i>ilvM</i>	4.73	1.07	6.16
<i>yifK</i>	3.15	1.04	5.48	<i>dadX</i>	4.78	0.81	8.27
<i>yciW</i>	3.19	1.08	6.67	<i>nrdD</i>	4.89	0.80	2.68
<i>thiH</i>	3.22	0.40	0.62	<i>napB</i>	4.97	1.00	6.00
<i>metH</i>	3.26	0.90	5.89	<i>sdhB</i>	5.06	1.14	6.34
<i>glpF</i>	3.28	0.87	5.41	<i>mdh</i>	5.08	1.03	5.93
<i>cbl</i>	3.33	1.19	6.89	<i>maeB</i>	5.12	0.93	5.51
<i>psiE</i>	3.35	0.86	5.75	WT	5.19	0.88	6.11
<i>tauA</i>	3.40	0.91	7.22	<i>glpD</i>	5.25	0.93	5.46
<i>ycgZ</i>	3.41	1.19	7.20	<i>ylaC</i>	5.42	1.05	6.10
<i>yfiM</i>	3.47	0.68	6.22	<i>ydcN</i>	5.53	1.07	6.19
<i>ybiJ</i>	3.64	0.88	3.06	<i>acnA</i>	5.63	1.19	6.59
<i>ilvG</i>	3.70	1.05	5.64	<i>fdnI</i>	5.89	1.04	4.51
<i>yqhA</i>	3.73	0.85	5.55	<i>yhjE</i>	5.94	0.89	5.90
<i>hslU</i>	3.77	0.81	5.14	<i>ynaJ</i>	6.10	0.96	5.08
<i>ssuE</i>	3.77	0.91	11.80	<i>deaD</i>	6.15	1.14	6.28
<i>proP</i>	3.82	0.99	5.41	<i>osmB</i>	6.23	0.97	5.68
<i>fdoI</i>	3.87	0.93	5.91	<i>yeeE</i>	6.27	0.90	5.75
<i>pdhR</i>	3.91	1.08	5.45	<i>clpA</i>	6.30	0.76	6.12
<i>cyoD</i>	3.96	1.07	6.91	<i>cyoE</i>	6.49	0.96	5.30
<i>gcd</i>	3.99	1.32	7.64	<i>intF</i>	6.58	1.13	6.45
<i>aceA</i>	4.00	1.09	6.28	<i>glpE</i>	6.82	1.14	6.74
<i>yzgL</i>	4.02	1.15	6.54	<i>tauB</i>	6.86	0.80	5.52
<i>ybiC</i>	4.03	0.86	7.59	<i>aceB</i>	6.98	0.99	5.33
<i>yceI</i>	4.05	0.88	5.47	<i>bhsA</i>	7.18	1.00	6.49
<i>fdnG</i>	4.07	1.11	5.36	<i>ylbA</i>	7.49	1.07	6.12
<i>msrB</i>	4.21	0.87	5.92	<i>fumA</i>	7.55	1.08	6.28
<i>yebZ</i>	4.24	0.89	5.44	<i>pgm</i>	8.81	0.91	4.99

Table S1. *E. coli* cultures were started in minimal medium with fumarate and sub-cultured into medium with nitrate (10 mM) for 6 hrs. Nitrosylation was measured by photolysis/chemiluminescence. Growth and nitrite levels were measured at A600 and by Griess assay respectively (n=3 to 21).

Table S2. Hcp-independent S-nitrosylation of Proteins During ARN, Related to Figure 3

Protein	Uniprot	Fold change WT	Fold change Δhcp	WT/Δhcp	Interact with Hcp
KatG Catalase-peroxidase	P13029	2.2	1.9	1.1	Y
CysJ Sulfite reductase [NADPH] flavoprotein alpha-component	P38038	3.2	2.9	1.1	
PurA Adenylosuccinate synthetase	P0A7D4	2.0	1.8	1.1	Y
CarA Carbamoyl-phosphate synthase small chain	P0A6F1	3.2	3.0	1.1	
GltD Glutamate synthase [NADPH] small chain	P09832	2.1	2.0	1.1	Y
InfB Translation initiation factor IF-2	P0A705	1.9	2.0	1.0	
FabB 3-oxoacyl-[acyl-carrier-protein] synthase 1	P0A953	2.3	2.4	1.0	
HchA Molecular chaperone Hsp31 and glyoxalase 3	P31658	2.2	2.5	0.9	
FabZ 3-hydroxyacyl-[acyl-carrier-protein] dehydratase	P0A6Q6	4.6	5.9	0.8	
Hcp Hydroxylamine reductase	P75825	16.4			

Table S2. Proteins that are S-nitrosylated during ARN in WT were identified as proteins that were pulled down by SNO-RAC ≥ 1.5 fold on nitrate versus fumarate. Proteins listed are S-nitrosylated comparably in WT and Δhcp . Proteins present in the Hcp interactome (Table S3) are identified with Y.

Table S3. Nitrate-dependent Hcp Interactome, Related to Figure 3

Protein	Uniprot	Protein	Uniprot
NarG Respiratory nitrate reductase 1 alpha chain	P09152	MetE 5-methyltetrahydropteroyltryglutamate	P25665
IlvB Acetolactate synthase isozyme 1 large subunit	P08142	GltD Glutamate synthase [NADPH] small chain	P09832
MiaB tRNA-2-methylthio-N(6)-dimethylallyl-adenosine synthase	P0AE11	MetA Homoserine O-succinyltransferase	P07623
OmpA Outer membrane protein A	P0A910	Gcp tRNA N6-adenosine threonylcarbamoyltransferase	P05852
AccD Acetyl-coenzyme A carboxylase carboxyl transferase	P0A9Q5	YcfP UPF0227 protein	P0A8E1
LpdA Dihydrolipoyl dehydrogenase	P0A9P0	DeaD ATP-dependent RNA helicase	P0A9P6
AsnB Asparagine synthetase B	P22106	AccA Acetyl-coenzyme A carboxylase carboxyl transferase	P0ABD5
EttA Energy-dependent translational throttle protein	P0A9W3	DnaB Replicative DNA helicase	P0ACB0
RplN 50S ribosomal protein L14	P0ADY3	PurA Adenylosuccinate synthetase	P0A7D4
PyrG CTP synthase	P0A7E5	IspG 4-hydroxy-3-methylbut-2-en-1-yl diphosphate synthase	P62620
IlvI Acetolactate synthase isozyme 3 large subunit	P00893	Hcr NADH oxidoreductase	P75824
NirB Nitrite reductase (NADH) large subunit	P08201	AroG Phospho-2-dehydro-3-deoxyheptonate aldolase	P0AB91
GapA Glyceraldehyde-3-phosphate dehydrogenase A	P0A9B2	GyrB DNA gyrase subunit B	P0AES6
SurA Chaperone	P0ABZ6	DnaK Chaperone protein	P0A6Y8
SecD Protein translocase subunit	P0AG90	AceF Dihydrolipoyllysine-residue acetyltransferase (PyrDH complex)	P06959
MetL Bifunctional aspartokinase/homoserine	P00562	RpoA DNA-directed RNA polymerase subunit alpha	P0A7Z4
AceE Pyruvate dehydrogenase E1 component	P0AFG8	CysC Adenylyl-sulfate kinase	P0A6J1
IlvA L-threonine dehydratase biosynthetic	P04968	AroF Phospho-2-dehydro-3-deoxyheptonate aldolase	P00888
MurC UDP-N-acetylmuramate--L-alanine ligase	P17952	AccC Biotin carboxylase	P24182
OppF Oligopeptide transport ATP-binding protein	P77737	MreB Rod shape-determining protein	P0A9X4
RpsG 30S ribosomal protein S7	P02359	MetF 5,10-methylenetetrahydrofolate reductase	P0AEZ1
RplE 50S ribosomal protein L5	P62399	Pur7 Phosphoribosylaminoimidazole-succinocarboxamide synthase	P0A7D7
GpmI 2,3-bisphosphoglycerate-independent phosphoglycerate mutase	P37689	ArgB Acetylglutamate kinase	P0A6C8
CysH Phosphoadenosine phosphosulfate reductase	P17854	ClpX ATP-dependent Clp protease ATP-binding subunit	P0A6H1
Upp Uracil phosphoribosyltransferase	P0A8F0	LeuC 3-isopropylmalate dehydratase large subunit	P0A6A6
FtsZ Cell division protein	P0A9A6	EF-Tu1 Elongation factor Tu 1	P0CE47
OmpR Transcriptional regulatory protein	P0AA16	TtcA tRNA 2-thiocytidine biosynthesis protein	P76055
MinD Septum site-determining protein	P0AEZ3	ObgE GTPase CgtA	P42641

NusG Transcription termination/antitermination protein	P0AFG0	LysC Lysine-sensitive aspartokinase 3	P08660
Rho Transcription termination factor	P0AG30	IivC Ketol-acid reductoisomerase	P05793
RplF 50S ribosomal protein L6	P0AG55	Tpx Thiol peroxidase	P0A862
RecA Protein RecA	P0A7G6	NarL Nitrate/nitrite response regulator protein	P0AF28
RplJ 50S ribosomal protein L10	P0A7J3	NarH Respiratory nitrate reductase 1 beta chain	P11349
RpsE 30S ribosomal protein S5	P0A7W1	IivH Acetolactate synthase isozyme 3 small subunit	P00894
RpsB 30S ribosomal protein S2	P0A7V0	OmpF Outer membrane protein F	P02931
RpsC 30S ribosomal protein S3	P0A7V3	DnaJ Chaperone protein	P08622
RpsK 30S ribosomal protein S11	P0A7R9	LeuA L-isopropylmalate synthase	P09151
ArgG Argininosuccinate synthase	P0A6E4	ArgA Amino-acid acetyltransferase	P0A6C5
Tsf Elongation factor Ts	P0A6P1	HslU ATP-dependent protease ATPase subunit	P0A6H5
HisD Histidinol dehydrogenase	P06988	PyrI Aspartate carbamoyltransferase regulatory chain	P0A7F3
RplM 50S ribosomal protein L13	P0AA10	RplK 50S ribosomal protein L11	P0A7J7
PyrB Aspartate carbamoyltransferase catalytic chain	P0A786	RplS 50S ribosomal protein L19	P0A7K6
GlyQ Glycine--tRNA ligase alpha subunit	P00960	RplI 50S ribosomal protein L9	P0A7R1
GatY D-tagatose-1,6-bisphosphate aldolase subunit	P0C8J6	RpsJ 30S ribosomal protein S10	P0A7R5
TrpG Bifunctional protein	P00904	RpsD 30S ribosomal protein S4	P0A7V8
GuaA GMP synthase [glutamine-hydrolyzing]	P04079	Tig Trigger factor	P0A850
TyrR Transcriptional regulatory protein	P07604	PflA Pyruvate formate-lyase 1-activating enzyme	P0A9N4
RplT 50S ribosomal protein L20	P0A7L3	ArcA Aerobic respiration control protein	P0A9Q1
HflK Modulator of FtsH protease	P0ABC7	FdnH Formate dehydrogenase, nitrate-inducible, iron-sulfur subunit	P0AAJ3
SucB Dihydrodipolyllysine-residue succinyltransferase component of 2-	P0AFG6	FabG 3-oxoacyl-[acyl-carrier-protein] reductase	P0AEK2
IbpB Small heat shock protein	P0C058	NtrC Nitrogen regulation protein NR(I)	P0AFB8
FdnG Formate dehydrogenase, nitrate-inducible, major subunit	P24183	SecY Protein translocase subunit	P0AGA2
RplB 50S ribosomal protein L2	P60422	CysA Sulfate/thiosulfate import ATP-binding protein	P16676
Aas Bifunctional protein	P31119	ThiE Thiamine-phosphate synthase	P30137
AcnB Aconitate hydratase 2	P36683	RavA ATPase	P31473
KatG Catalase-peroxidase	P13029	RplD 50S ribosomal protein L4	P60723
		YdgH Protein YdgH	P76177

Table S3. The Hcp interactome was identified following ARN for 1 hr (n=3) or 6 hr (n=3) using the criteria described in Materials and Methods. Proteins listed were identified at least twice at either of the two time points. Proteins that are also S-nitrosylated in an Hcp-dependent manner are indicated in red.

Table S4. NO-dependent Hcp Interactome, Related to Figure 3

Protein	Uniprot	Nitrate interactome
OppD Oligopeptide transport ATP-binding protein	P76027	
YdiJ Uncharacterized protein	P77748	
IspG 4-hydroxy-3-methylbut-2-en-1-yl diphosphate synthase	P62620	Y
MetG Methionyl-tRNA synthetase	P00959	
GltD Glutamate synthase [NADPH] small chain	P09832	Y
GltB Glutamate synthase [NADPH] large chain	P09831	
FdhF Formate dehydrogenase H	P07658	
CysI Sulfite reductase [NADPH] hemoprotein beta-component	P17846	
AceE Pyruvate dehydrogenase E1 component	P0AFG8	Y
Aas Bifunctional protein	P31119	Y
NuoC NADH-quinone oxidoreductase subunit C/D	P33599	
KatG Catalase-peroxidase	P13029	Y
MetE 5-methyltetrahydropteroyltriglutamate--homocysteine methyltransferase	P25665	Y
CysN Sulfate adenylyltransferase subunit 1	P23845	
AccA Acetyl-coenzyme A carboxylase carboxyl transferase subunit alpha	P0ABD5	Y
MiaB tRNA-2-methylthio-N(6)-dimethylallyl-adenosine synthase	P0AEI1	Y
OppF Oligopeptide transport ATP-binding protein	P77737	Y
TrpG Bifunctional protein	P00904	Y
MetH Methionine synthase	P13009	
AccD Acetyl-coenzyme A carboxylase carboxyl transferase subunit beta	P0A9Q5	Y
MbhL Hydrogenase-1 large chain	P0ACD8	
UspA Universal stress protein A	P0AED0	
ProB Glutamate 5-kinase	P0A7B5	
LeuC 3-isopropylmalate dehydratase large subunit	P0A6A6	Y
GatY D-tagatose-1,6-bisphosphate aldolase subunit	P0C8J6	Y
NuoG NADH-quinone oxidoreductase subunit G	P33602	
AceF Dihydrolipoyllysine-residue acetyltransferase component of pyruvate dehydrogenase complex	P06959	Y
IivC Ketol-acid reductoisomerase	P05793	Y
LpdA Dihydrolipoyl dehydrogenase	P0A9P0	Y
SucA 2-oxoglutarate dehydrogenase E1 component	P0AFG3	

Table S4. The Hcp interactome was identified following treatment with DEANO (100 μ M, 10 min.) using the criteria described in Materials and Methods. Proteins listed were identified in at least 2 independent experiments. Proteins present in the nitrate-dependent Hcp interactome (Table S3) are identified with Y.

Table S5. Primers Used for Cloning and QPCR, Related to STAR Methods

Primer name	Primer sequence
Hcp-pUC19-F	ATTAGGATCCTTTAAGAAGGAGATATACATATGTTTTGTGTGCAATG
Hcp-pUC19-R	CGATCAAGCTTTTACTTGTTCATCGTCGTCCTTGTAGTCCGCGCTCAACAGTTGC
OxyR-pUC19-F	ATTAGGATCCCTTTAAGAAGGAGATATACATATGAATATTCG
OxyR-pUC19-R	GCATAAGCTTTTACTTGTTCATCGTCGTCCTTGTAGTCAACCGCCTGTTTTAAAAC
LpdA-pUC19-F	ATTAGGATCCTTTAAGAAGGAGATATACATATGAGTACTGAAATCAAAACTC
LpdA-pUC19-R	CGATCAAGCTTTTACTTGTTCATCGTCGTCCTTGTAGTCCCTTCTTCTTCGCTTTCG
Hcp-pET21b-F	ATATACATATGTTTTGTGTGCAATGTGAACAAAC
Hcp-pET21b-R	TAATAAGCTTCGCGCTCAACAGTTGCTTCATG
Hcr-pET21b-F	ATATACATATGACGATGCCAACGAATC
Hcr-pET21b-R	ATTGCAAGCTTTGCGGAGAACCAAATCC
OxyR-pET21b-F	ACTATCATATGAATATTCGTGATCTTG
OxyR-pET21b-R	TGAATCTCGAGAACCGCCTGTTTTAAAACCTTATCG
LpdA-pET21b-F	ATCATAACATATGAGTACTGAAATCAAAACTCAGG
LpdA-pET21b-R	GACTGAAAGCTTCTTCTTCTTCGCTTTCGGGTTTCGG
GapA-pET21b-F	ATCATAACATATGACTATCAAAGTAGGTATCAACG
GapA-pET21b-R	GACTGAAAGCTTTTTGGAGATGTGAGCGATCAGG
CodA-pET21b-F	ATCATAGCTAGCGTGTGCAATA ACGCTTTACA AACAATTATT AACG
CodA-pET21b-R	GACTGAAAGCTTACGTTTGTAATCGATGGCTTCTGG
NapA-pET21b-F	ATCATAGCTAGCATGAAACTCA GTCGTCGTAG CTTTATGAAA GC
NapA-pET21b-R	GACTGAAAGCTTCACCTTCTCCAGTTTGACCGCGC
hcp-F (QPCR)	TGACCTTCAGGATTTACTCATCGCGG
hcp-R (QPCR)	GATGATGCCGTATTCACGCGCTTT

SUPPLEMENTAL FIGURE LEGENDS

Figure S1. Induction of *hcp* and Comparison of SNO-proteins Between WT and Δhcp During ARN, Related to Figure 1 and Figure 3

(A) Cells were grown anaerobically on nitrate or fumarate prior to RNA extraction and QPCR. Fold-expression of *hcp* on nitrate was calculated relative to expression on fumarate using the comparative C_t method. Expression in each sample was normalized to that of 16s rRNA (n=3, \pm SEM).

(B) *E. coli* were grown anaerobically in minimal media containing either fumarate or nitrate (10 mM) for 6 hr and lysates were subjected to SNO-RAC followed by SDS-PAGE and Coomassie staining. Representative gel, n=4.

Figure S2. SNO-dependent Intramolecular Disulfide Formation in Hcp *In Vitro* and *In Vivo*, Related to Figure 3

(A) Hcp (1.8 μ M) was treated anaerobically with CysNO (200 μ M), followed by SDS-PAGE and Coomassie staining. As for exposure to NO (Figure 3B), exposure to the S-nitrosylating agent CysNO resulted in a decrease in m_r in non-reduced samples, indicative of disulfide formation, which was reversed by reduction. Representative gel, n=2.

(B) The decrease in m_r of Hcp induced by anaerobic treatment with NO (DEANO, 200 μ M, 10 min) was diminished when ascorbate (Asc) was included in the reaction mixture as a selective reductant of SNO, and was eliminated when glutathione (GSH) was included as a reductant of SNO and disulfide. Representative gel, n=2.

(C) Hcp was treated anaerobically with DEANO for 5 min, and Hcr (1.8 μ M) and NADH (100 μ M) were added to an aliquot for an additional 10 min. The NO-induced decrease in m_r is substantially diminished by Hcr+NADH, consistent with Hcr-catalyzed disulfide reduction

with NADH as co-factor. Representative gel, n=3. Dashed lines indicate in-gel cuts for clarity.

(D) Hcp dimerization and interactome formation *in vivo* occur rapidly during ARN. WT/HcpF were grown in the presence of either nitrate or fumarate (10 mM). Lysates were analyzed by SDS-PAGE. Hcp was visualized by Western blotting with anti-FLAG antibody. Representative gel, n=2.

(E) MS/MS (LC-MS/MS) spectra of the disulfide bond formed between Cys102-Cys155 in Hcp during ARN. A representative annotated MS/MS fragmentation spectrum is shown illustrating the Cys102- and Cys155-containing peptides (labeled as A and B respectively) with disulfide bond between Cys102-155. Peptide sequences are shown at the top of the spectrum, with the annotation of the identified matched amino-terminus containing ions (*b* ions) in black and the carboxyl terminus ions (*y* ions) in red. For clarity, only major identified peaks are labeled.

(F) Dimerization and interactome formation by Hcp is abrogated under reducing conditions. As in Figure 3C, WT *E. coli* overexpressing FLAG-tagged Hcp (WT/HcpF) were grown anaerobically either in nitrate (10 mM, 6 hr), or in fumarate followed by treatment with DEANO (100 μ M). Lysates were analyzed by reducing SDS-PAGE and Hcp was visualized by Western blotting with anti-FLAG antibody. Representative gel, n=3.

(G) WT, Δhcp , Δhcp /HcpF, Δhcp /HcpF C102/155S were grown anaerobically in LB medium in the presence of nitrate (10 mM, 2.5 hrs) and SNO levels were measured by Hg²⁺-coupled photolysis/chemiluminescence (n=5, \pm SEM). * differs from Δhcp /HcpF, p < 0.05.

Figure S3. Trans-nitrosylases Propagate Hcp-dependent S-nitrosylation, Related to Figure 4

(A) TrxA (4.8 μ M) was treated with DEANO (50 μ M) in the presence or absence of Hcp (1.2 μ M) as indicated for 15 min at room temperature under anaerobic conditions. The reactions were subjected to SNO-RAC and TrxA was visualized by Western blotting using anti-thioredoxin antibody (n=2).

(B) CodA (1.6 μ M) or OxyR (1.6 μ M) was treated with DEANO (50 μ M) and Hcp (200 nM) anaerobically *in vitro*. S-nitrosylation of CodA and OxyR was assessed by SNO-RAC followed by western blotting and densitometry. The yield of SNO-protein (SNO-protein/total) was calculated and data are presented re SNO-OxyR (n=3, \pm SEM).

Figure S4. S-nitrosylation of LpdA and NarH During ARN is Decreased in the Absence of Hcp, Related to Figure 5

(A) WT/LpdA-FLAG and Δhcp /LpdA-FLAG cells were grown anaerobically on 10 mM nitrate. Lysates were analyzed by SNO-RAC (n= 3, \pm SEM). * differs from 2 hrs WT/LpdA-FLAG by ANOVA with Dunnett's test, $p < 0.05$.

(B) WT/NarH-FLAG, Δhcp /NarH-FLAG, and WT/NarH C184S-FLAG cells were grown anaerobically on nitrate (N) or fumarate (F) (10 mM, 6 hr). Lysates were analyzed by SNO-RAC (n=3, \pm SEM). * differs from nitrate grown WT/NarH-FLAG by ANOVA with Dunnett's test, $p < 0.05$.

Figure S5. Hcp Plays a Role in Protection from Nitrosative Stress, Related to Figure 5

(A) *E. coli* cultures were started in minimal medium including nitrate (10 mM) at A600 of 0.1. Where indicated sodium nitroprusside (NP; 2 mM) was added and cells were grown anaerobically for 6 hr. SNO levels were measured by Hg^{2+} -coupled photolysis/chemiluminescence (n=3, \pm SEM).

(B) *E. coli* cultures were started in minimal medium including 10 mM fumarate or 10 mM nitrate at A600 of 0.2. At various time points, cultures were fixed in 0.5% formaldehyde and A600 was measured (n=3, \pm SEM). * p<0.05 WT vs $\Delta hcp/\Delta norV$.